

Supplementary Information

For

Mechanistic investigation of the Zn/Pd/C catalyzed cleavage and hydrodeoxygenation of lignin

Table of Contents

Figure S1. ¹H NMR of 1-(4-Benzyloxy-3-methoxyphenyl)propane-1,3-diol (PG-diol) in (CD₃)₂CO

Figure S2. ¹H NMR of PG-diol (1-(4-hydroxy-3-methoxyphenyl)propane-1,3-diol) in (CD₃)₂CO.

Figure S3. ¹³C NMR of PG-diol (1-(4-hydroxy-3-methoxyphenyl)propane-1,3-diol) in (CD₃)₂CO.

Scheme S1. Effect of increased Zn^{II} loading in reaction of PG-diol with Pd/C and Zn(OAc)₂.
Reaction conditions: methanol solvent, 500 psig H₂, 150 °C, 8 hours.

Scheme S2. Reaction of PG-OH with Pd/C and Zn^{II}

Figure S4. GC chromatogram of products obtained from reaction of PG-diol with Pd/C as described in Scheme 4.1.

Figure S5. GC chromatogram of products obtained from reaction of PG-diol with Pd/C and Zn^{II} as described in Scheme 4.1.

Figure S6. HPLC/MS chromatogram of products obtained from reaction of PG-diol with Pd/C as described in Scheme 4.1.

Figure S7. HPLC/MS chromatogram of products obtained from reaction of PG-diol with Pd/C and Zn^{II} as described in Scheme 4.1.

Figure S8: HMQC of lignin model compound 1 in CD₃CN

Figure S9. HMQC lignin model compound and Zn(OTf)₂ (1:1 molar ratio) in CD₃CN.

Figure S10. Plot of normalized chemical shift of OH-A (model lignin compound 1) vs [Zn^{II}].

Figure S11. Plot of normalized chemical shift of OH-B (model lignin compound 1) vs [Zn^{II}].

Figure S12. GC chromatogram of lignin catalysis products obtained from poplar wood using Zn/Pd/C catalyst (Zn: Pd = 2:1 molar ratio).

Figure S13. GC chromatogram of lignin catalysis products obtained from poplar wood using Zn/Pd/C catalyst (Zn: Pd = 0.1:1 molar ratio).

Figure S14. GC chromatogram of lignin catalysis products obtained from poplar wood using Pd/C catalyst.

Equation for calculation of % Yield in Poplar reactions

Control reactions with lignin model compound 1

Figure S15. HPLC/MS of reaction products of lignin model compound 1 with $\text{Zn}(\text{OAc})_2 \cdot 2\text{H}_2\text{O}$.

Figure S16. HPLC/MS of reaction products reaction showing thermal decomposition of lignin model compound 1 in methanol.

Figure S17. HPLC/MS of reaction products reaction showing thermal decomposition of lignin model compound 1 treated with $\text{Zn}(\text{OAc})_2 \cdot 2\text{H}_2\text{O}$ at elevated temperatures.

Figure S18. ^1H NMR spectra of lignin model compound guaiacylglycerol- β -guaiacyl in CD_3CN .

Figure S 19. ^1H NMR spectra of lignin model compound guaiacylglycerol- β -guaiacyl in CD_3CN , with 1 equivalent $\text{Zn}(\text{OTf})_2$.

Table S1: Reaction of poplar biomass with Pd/C and Zn^{II} in ethanol solvent.

Figure S20. GC chromatogram of lignin catalysis products obtained from poplar wood using Pd/C catalyst in ethanol. Yields and reaction conditions reported in Table S1, entry 2.

Figure S21. GC chromatogram of lignin catalysis products obtained from poplar wood using Zn/Pd/C catalyst in ethanol. Yields and reaction conditions reported in Table S1, entry 1.

Figure S22: Van't Hoff Plot for binding of OH-A of lignin model compound to Zn^{II}

Figure S23: Van't Hoff Plot for binding of OH-B of lignin model compound to Zn^{II}

Preparation of PG-diol (1-(4-hydroxy-3-methoxyphenyl)propane-1,3-diol)

Preparation of PS-OH (4-(3-hydroxypropyl)-2,6-dimethoxyphenol)

HPLC/MS Analysis Procedures

Supplemental References

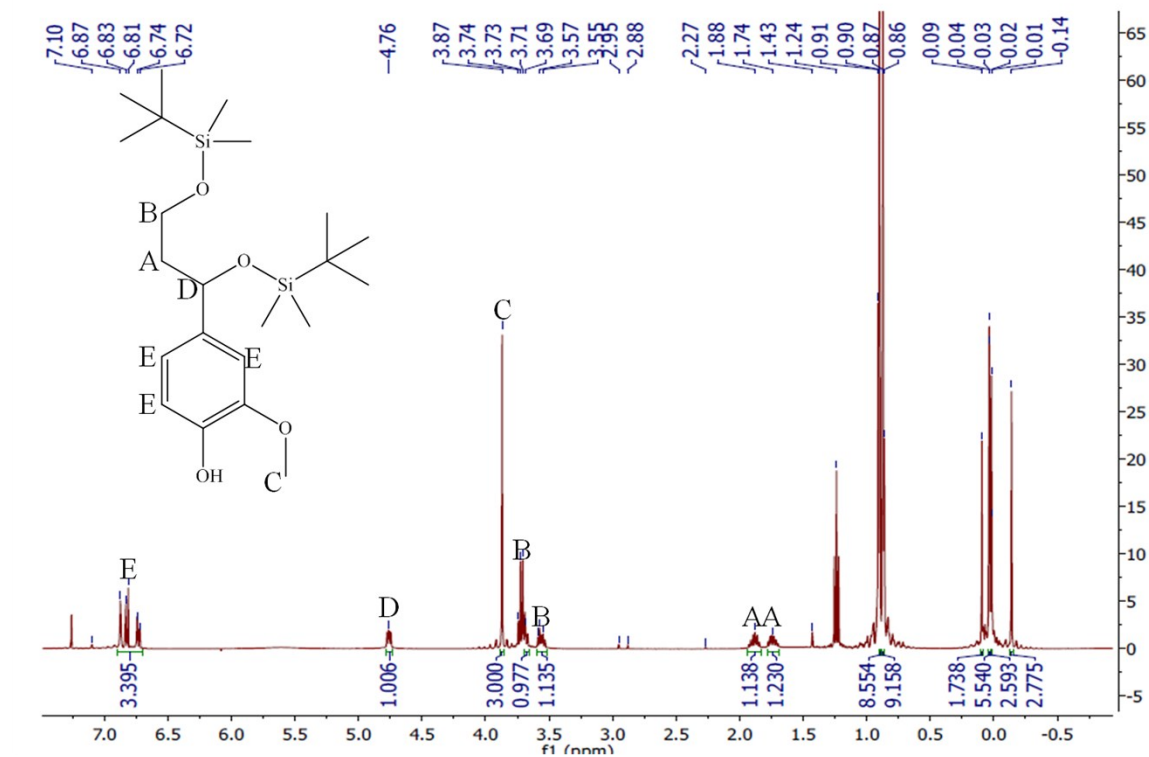


Figure S1. ¹H NMR of 1-(4-Benzyloxy-3-methoxyphenyl)propane-1,3-diol (PG-diol) in (CD₃)₂CO.

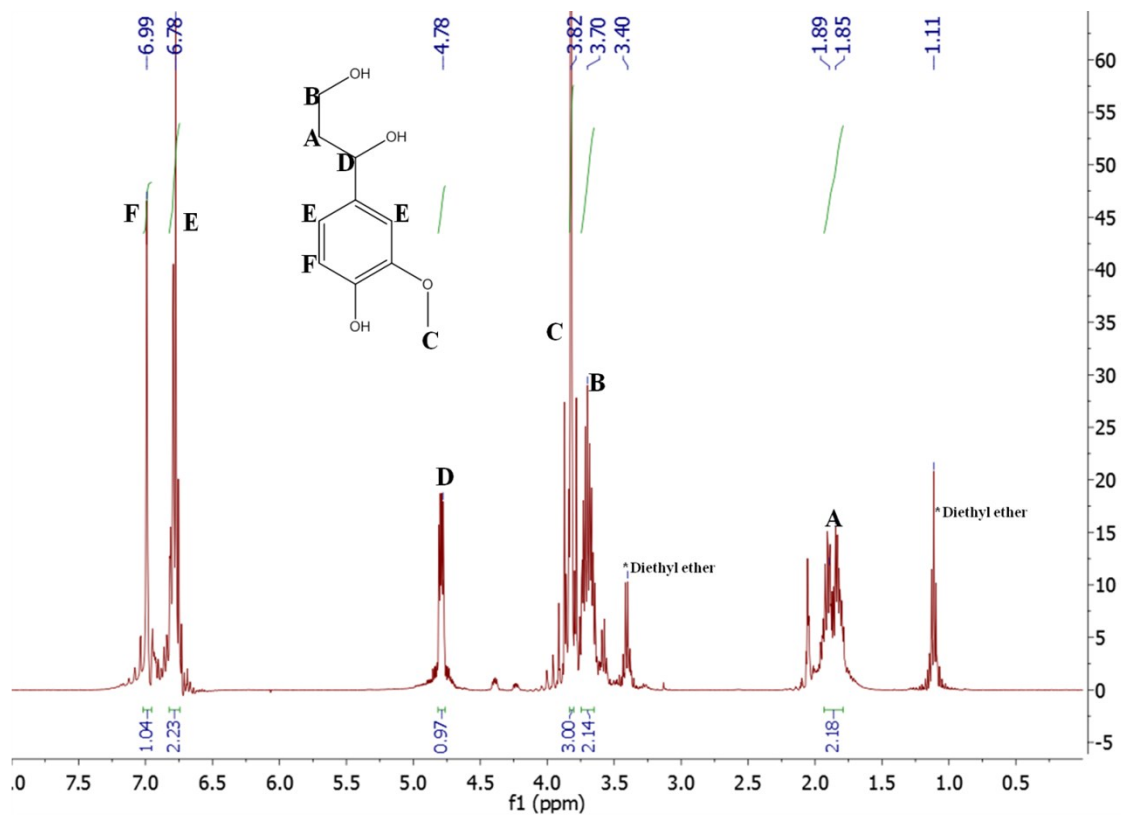


Figure S2. ^1H NMR of PG-diol (1-(4-hydroxy-3-methoxyphenyl)propane-1,3-diol) in $(\text{CD}_3)_2\text{CO}$.

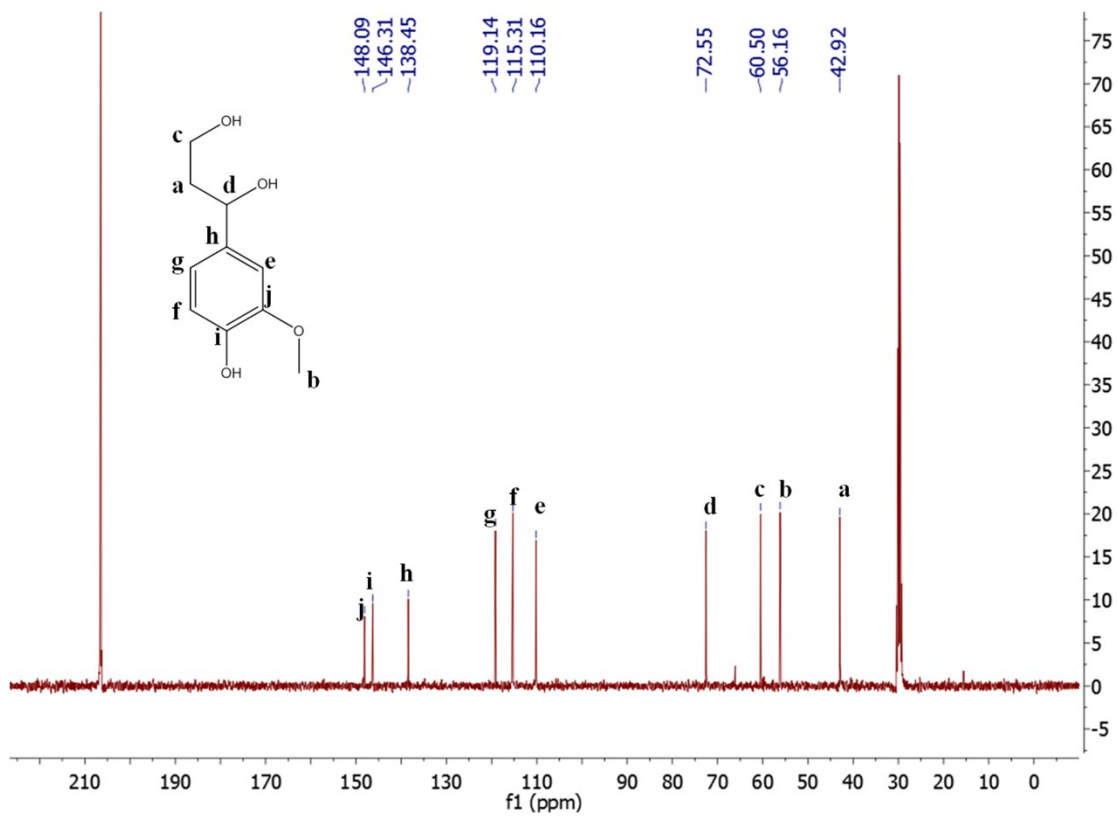
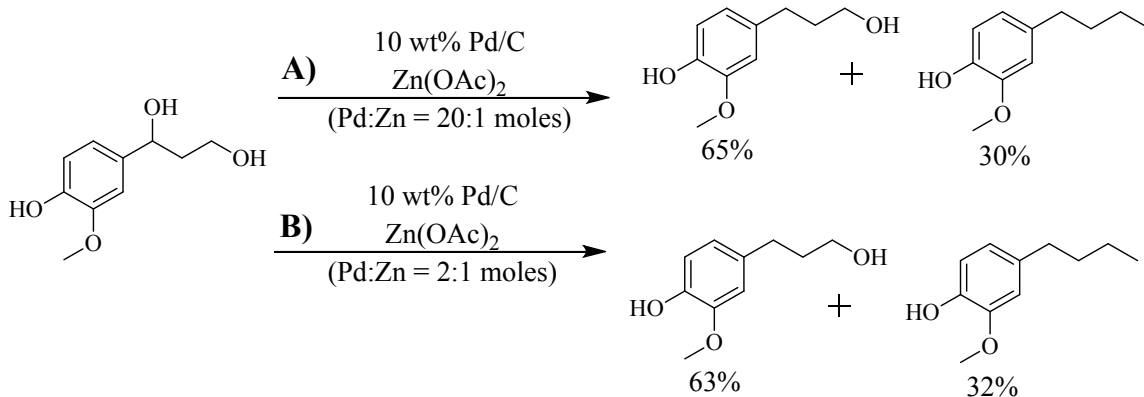
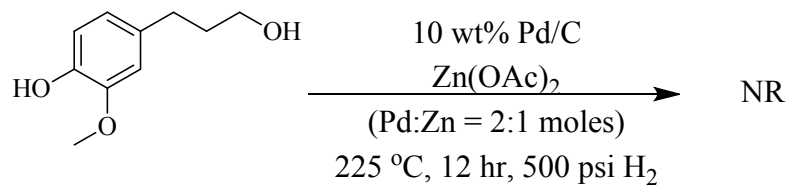


Figure S3. ^{13}C NMR of PG-diol (1-(4-hydroxy-3-methoxyphenyl)propane-1,3-diol) in $(\text{CD}_3)_2\text{CO}$.



Scheme S1. Effect of increased Zn^{II} loading in reaction of PG-diol with Pd/C and Zn(OAc)_2 . Reaction conditions: methanol solvent, 500 psig H_2 , 150 °C, 8 hours. Products analyzed by GC-FID.



Scheme S2. Reaction of PG-OH with Pd/C and Zn^{II} . Product analyzed by GC-FID.

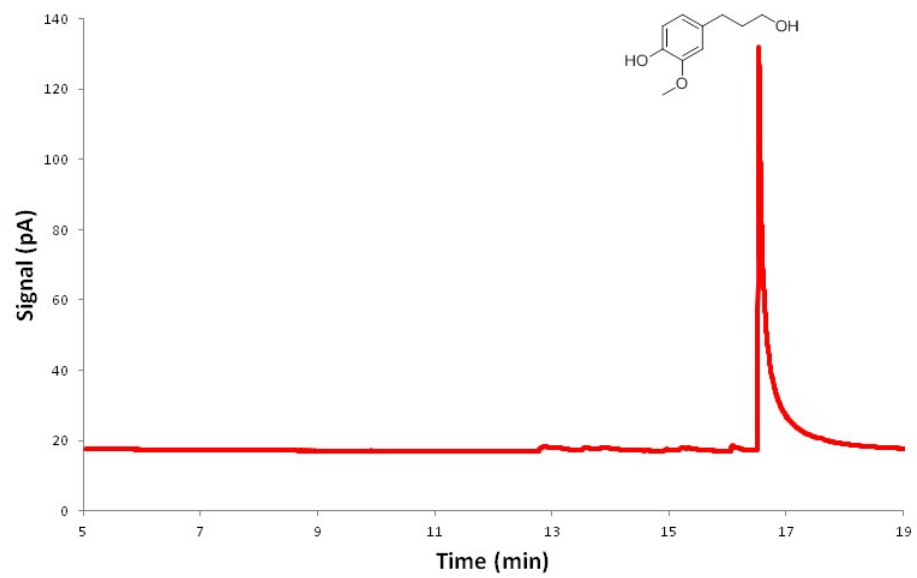


Figure S4. GC chromatogram of products obtained from reaction of PG-diol with Pd/C as described in Scheme 1.

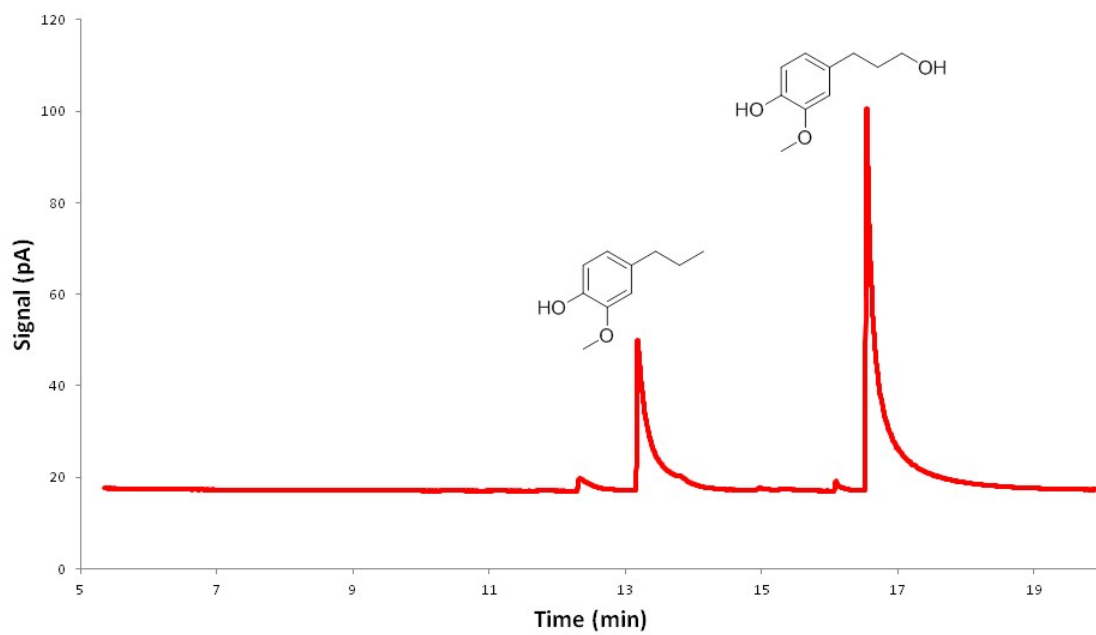


Figure S5. GC chromatogram of products obtained from reaction of PG-diol with Pd/C and Zn^{II} as described in Scheme 1.

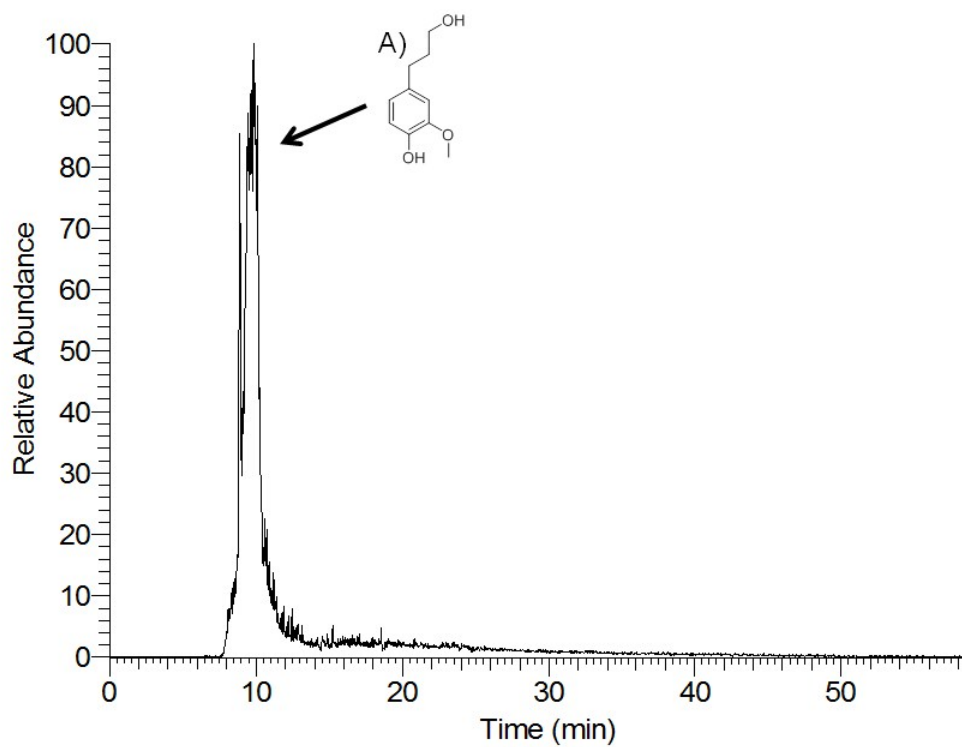


Figure S6: HPLC/MS selected ion chromatogram of products obtained from reaction of PG-diol with Pd/C as described in Scheme 4.1. Identified compounds: A) PG-OH

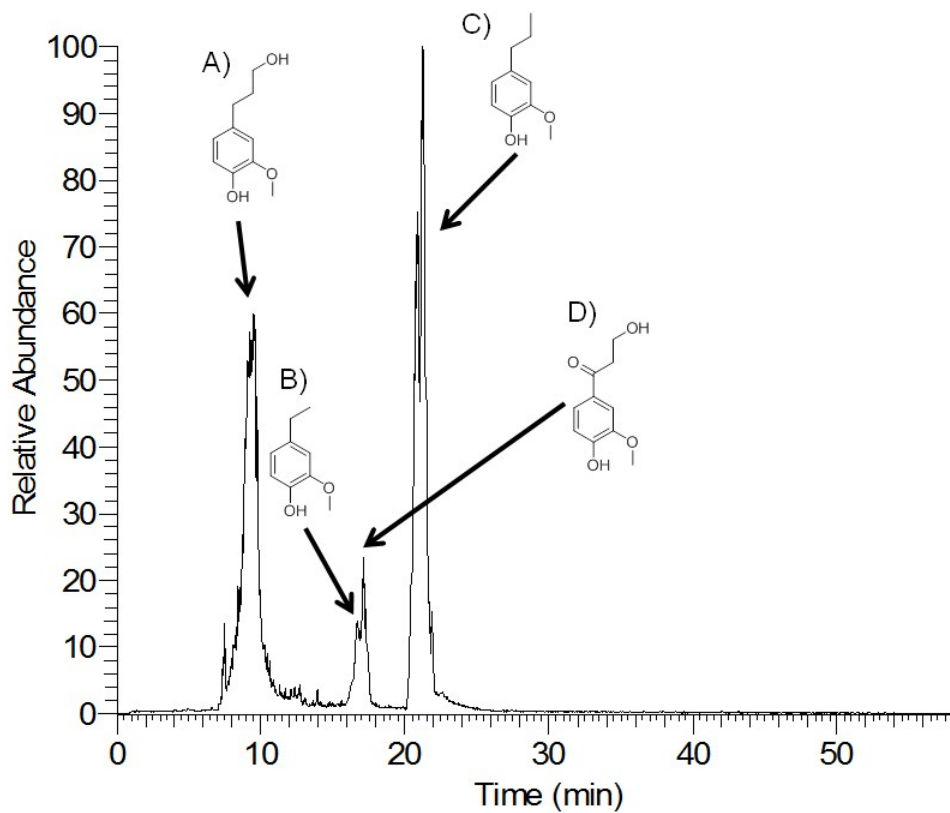


Figure S7: HPLC/MS selected ion chromatogram of products obtained from reaction of PG-diol with Pd/C and Zn^{II} as described in Scheme 4.1. Identified compounds:

- A) PG-OH
- B) 4-ethyl-2-methoxyphenol
- C) PG
- D) 3-hydroxy-1-(4-hydroxy-3-methoxyphenyl)propan-1-one

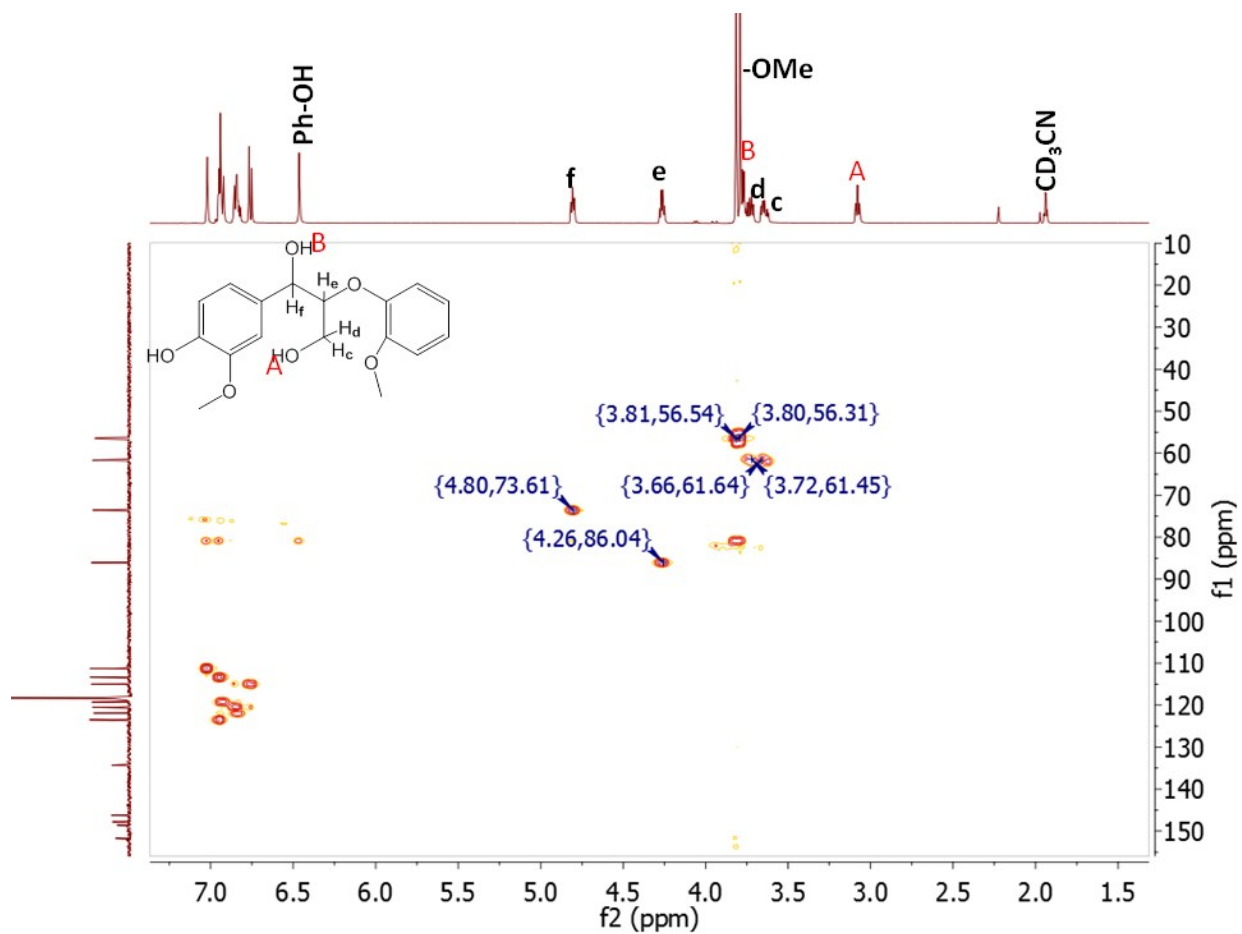


Figure S8: HMQC of lignin model compound 1 in CD₃CN.

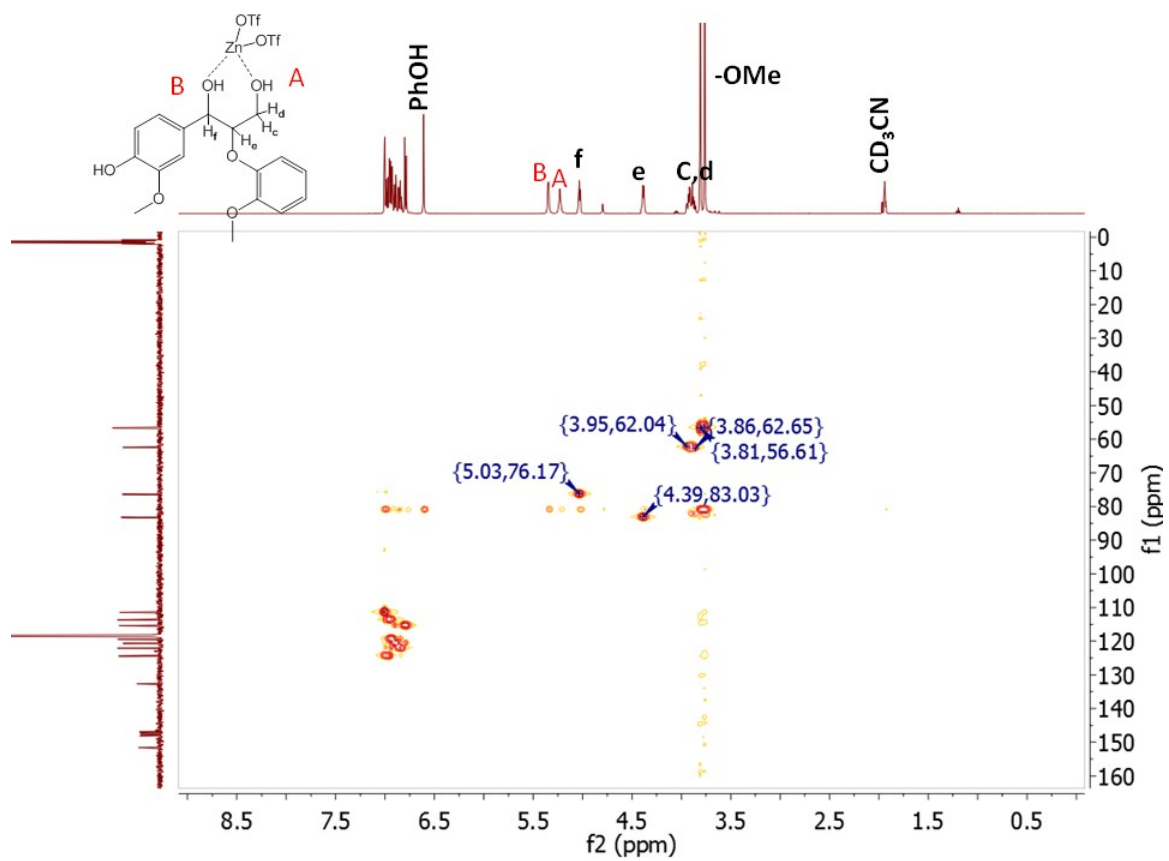


Figure S9. HMQC lignin model compound and Zn(OTf)₂ (1:1 molar ratio) in CD₃CN.

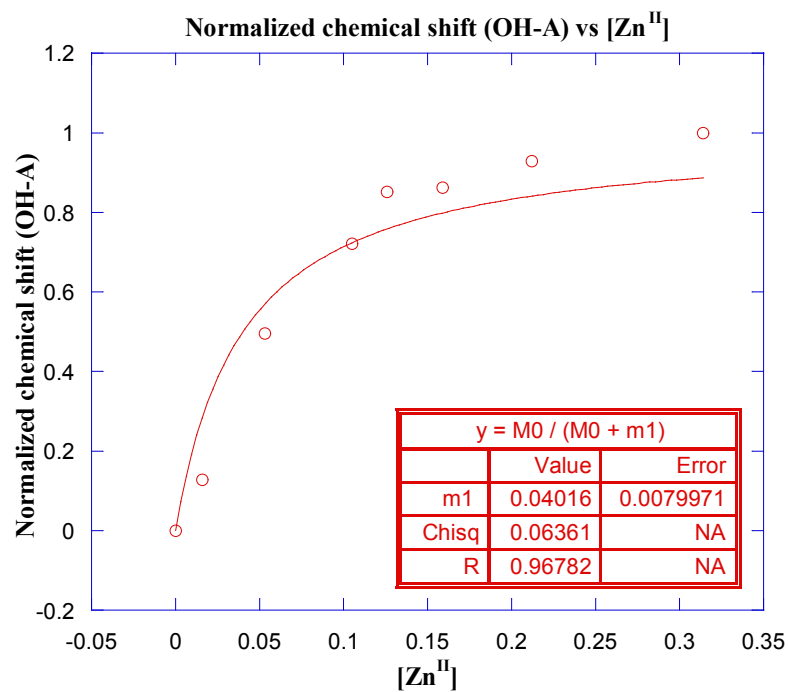


Figure S10: Plot of normalized chemical shift of OH-A (model lignin compound 1) vs [Zn^{II}]. Lignin model compound 1 dissolved in CD₃CN. Proton shift of OH(A) and OH(B) monitored by ¹H NMR as increasing equivalents of Zn(OTf)₂ added to solution, as illustrated in Figure 3. Normalized chemical shift derived using Equation 1. Plot generated using KaleidaGraph version 3.6.

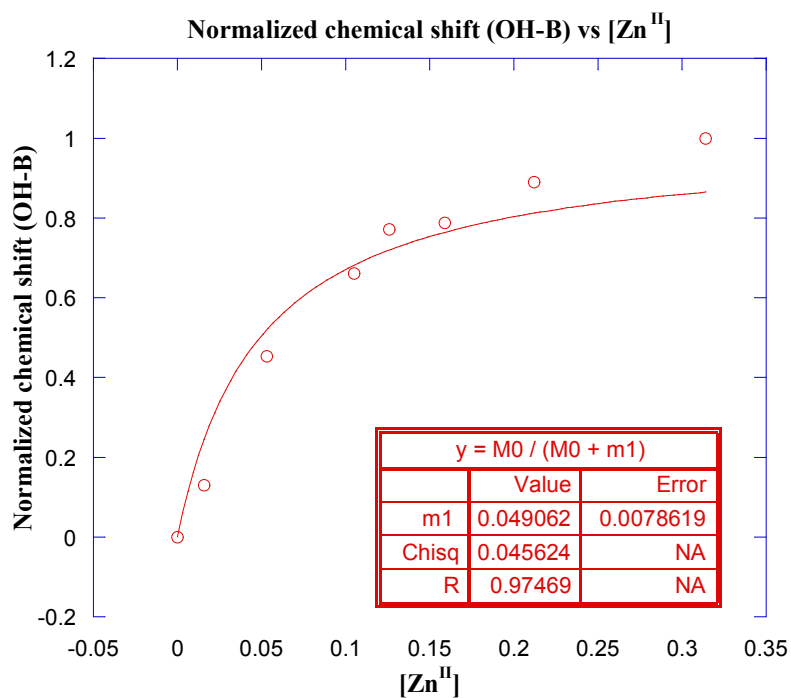


Figure S11: Plot of normalized chemical shift of OH-B (model lignin compound 1) vs $[Zn^{II}]$. Lignin model compound 1 dissolved in CD_3CN . Proton shift of OH(A) and OH(B) monitored by 1H NMR as increasing equivalents of $Zn(OTf)_2$ added to solution, as illustrated in Figure 3. Normalized chemical shift derived using Equation 1. Plot generated using KaleidaGraph version 3.6.

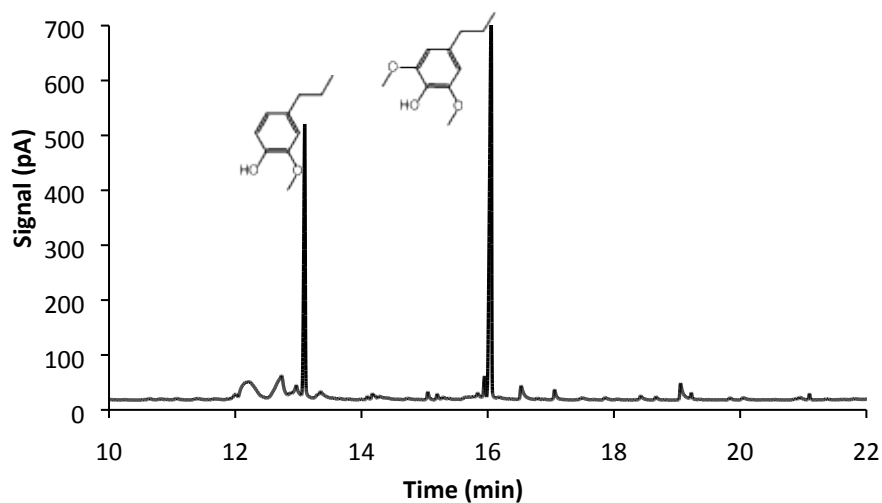


Figure S12. GC chromatogram of lignin catalysis products obtained from poplar wood using Zn/Pd/C catalyst, (Zn: Pd = 2:1 molar ratio). Yields and reaction conditions reported in Table 1, entry 2 of main text.

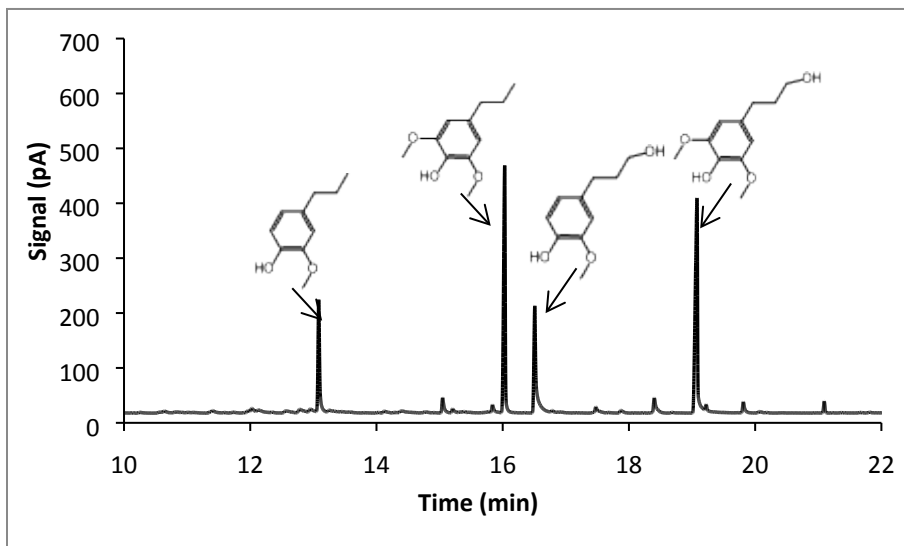


Figure S13. GC chromatogram of lignin catalysis products obtained from poplar wood using Zn/Pd/C catalyst (Zn: Pd = 0.1:1 molar ratio). Yields and reaction conditions reported in Table 1, entry 5 of main text.

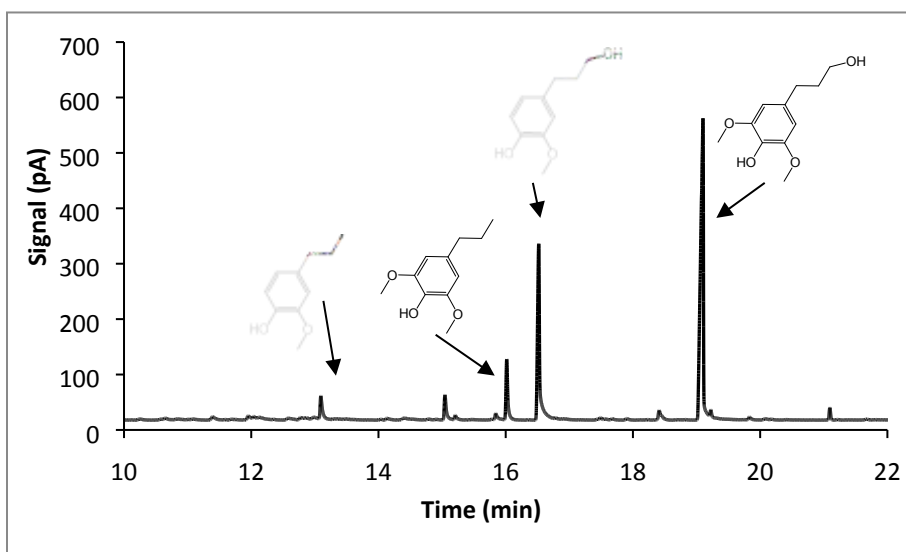


Figure S14. GC chromatogram of lignin catalysis products obtained from poplar wood using Pd/C catalyst.). Yields and reaction conditions reported in Table 1, entry 6 of main text.

Calculating % Yield in Poplar reactions

The % yield of products from poplar biomass (Table 1 of main text) is based on the total mass of the products and removed O divided by the mass of the lignin content of each sample as shown in the following equation. “Phenolic compounds” refers to PG, PS, PG-OH, and PS-OH.

$$\% \text{ yield} = \frac{\text{mass phenolic compounds (mg)} + \text{removed O (mg)}}{\text{initial weight of dry biomass (mg)} \times \text{ABSL lignin \%}} \times 100$$

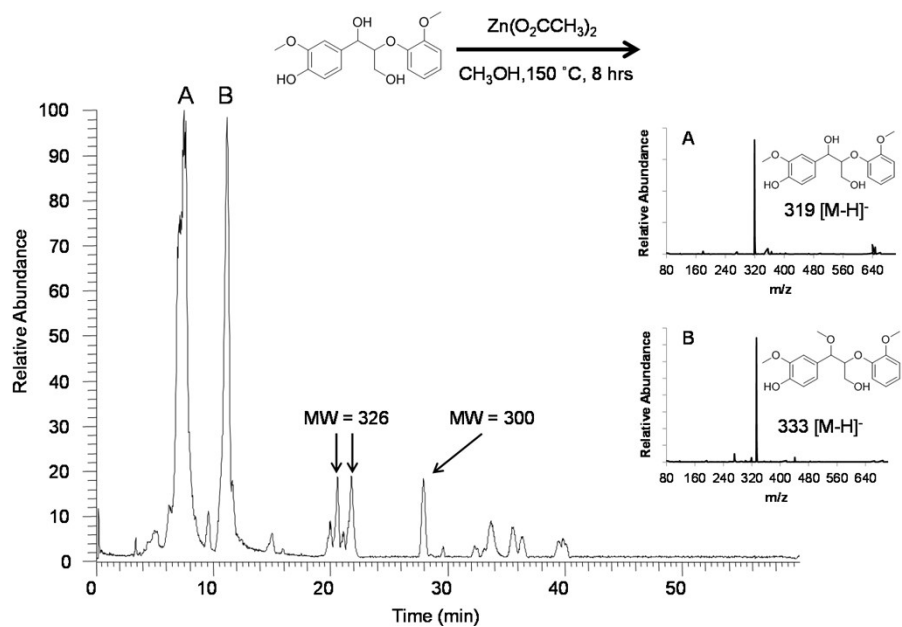


Figure S15. HPLC/MS of reaction products of lignin model compound 1 with $Zn(OAc)_2 \cdot 2H_2O$. Lignin model compound 1 dissolved in methanol along with 10 wt% $Zn(OAc)_2 \cdot 2H_2O$, pressurized with 300 psig H_2 , and heated at $150^\circ C$ for 8 hours. Solution was cooled to room temperature and analyzed by HPLC/MS as described below. Identified compounds:
 A) 1-(4-hydroxy-3-methoxyphenyl)-2-(2-methoxyphenoxy)propane-1,3-diol
 B) 4-(3-hydroxy-1-methoxy-2-(2-methoxyphenoxy)propyl)-2-methoxyphenol

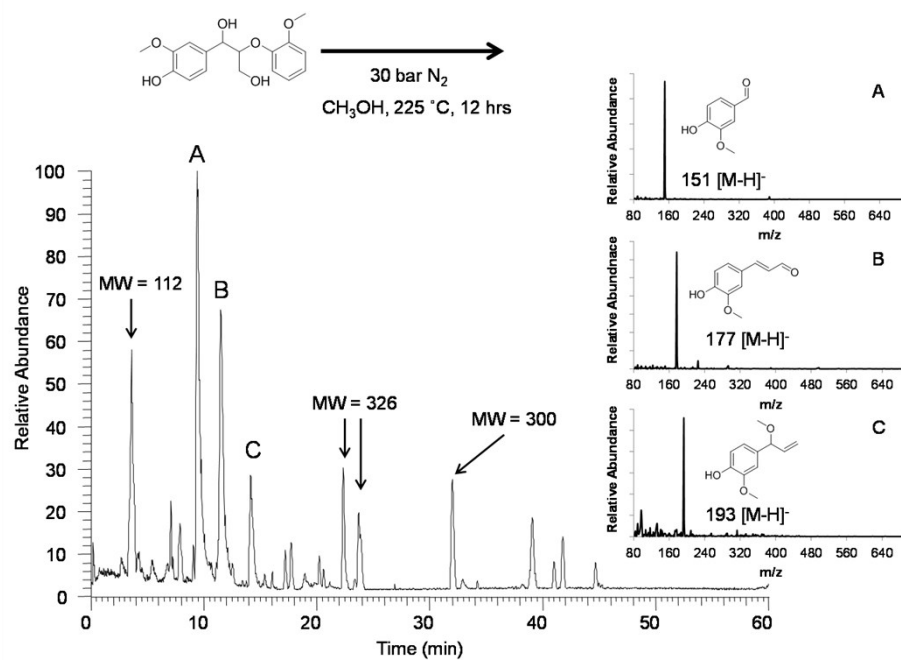


Figure S16. HPLC/MS of reaction products reaction showing thermal decomposition of lignin model compound 1 in methanol. Lignin model compound 1 dissolved in methanol, pressurized with 30 psig N₂, and heated at 225 °C for 12 hours. Solution was cooled to room temperature and analyzed by HPLC/MS as described below. Identified compounds:

- A) 4-hydroxy-3-methoxybenzaldehyde
- B) (E)-3-(4-hydroxy-3-methoxyphenyl)acrylaldehyde
- C) 2-methoxy-4-(1-methoxybut-3-en-1-yl)phenol

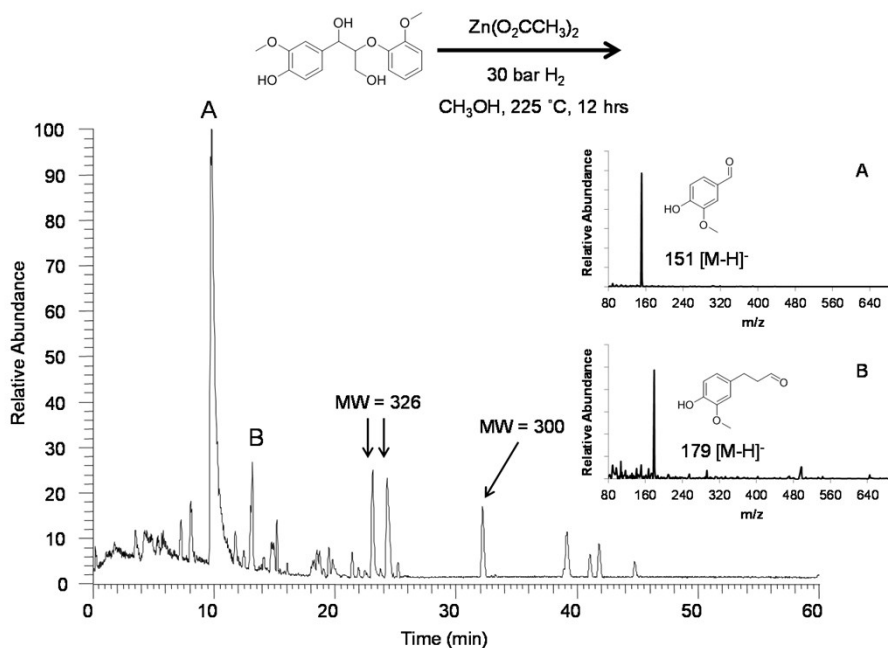


Figure S17. HPLC/MS of reaction products reaction showing thermal decomposition of lignin model compound 1 treated with $Zn(OAc)_2 \cdot 2H_2O$ at elevated temperatures. Lignin model compound 1 dissolved in methanol with 10 wt% $Zn(OAc)_2 \cdot 2H_2O$, pressurized with 434 psig H_2 , and heated at 225 °C for 12 hours. Solution was cooled to room temperature and analyzed by HPLC/MS as described below. Identified compounds:

- A) 4-hydroxy-3-methoxybenzaldehyde
- B) 3-(4-hydroxy-3-methoxyphenyl)propanal

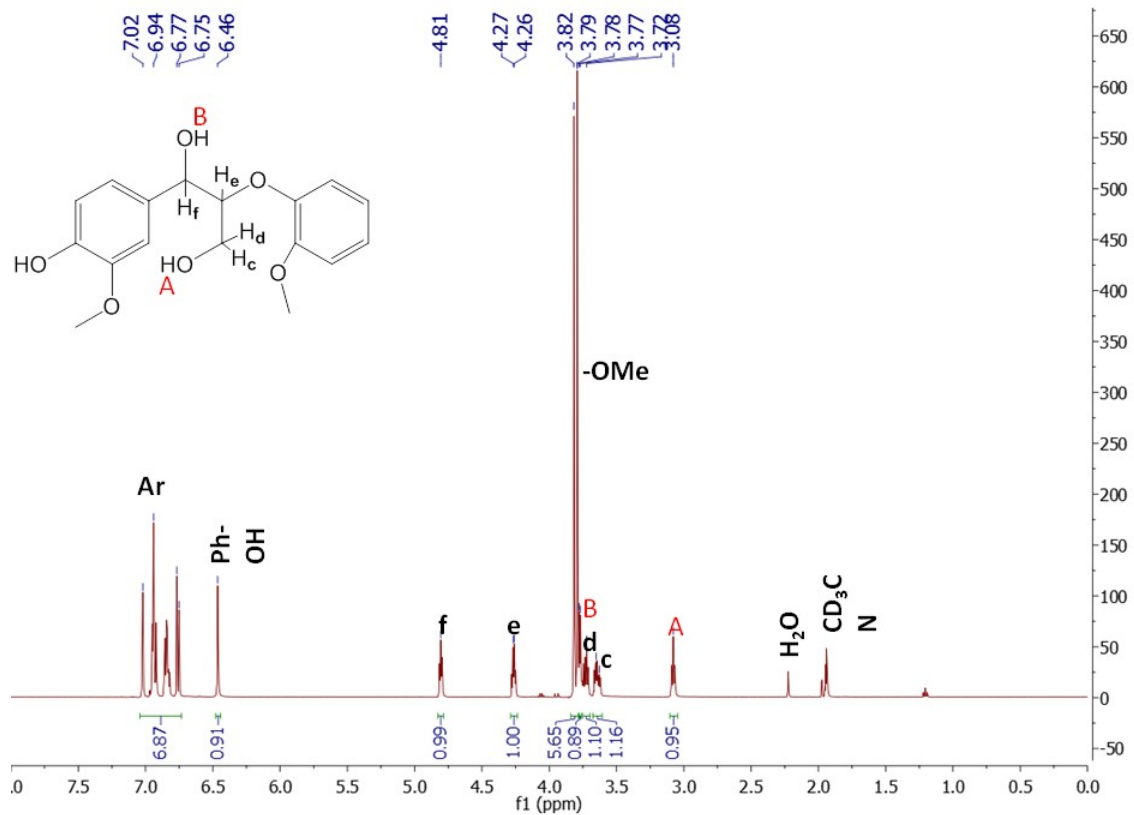


Figure S18. ^1H NMR spectra of lignin model compound guaiacylglycerol- β -guaiacyl in CD_3CN .

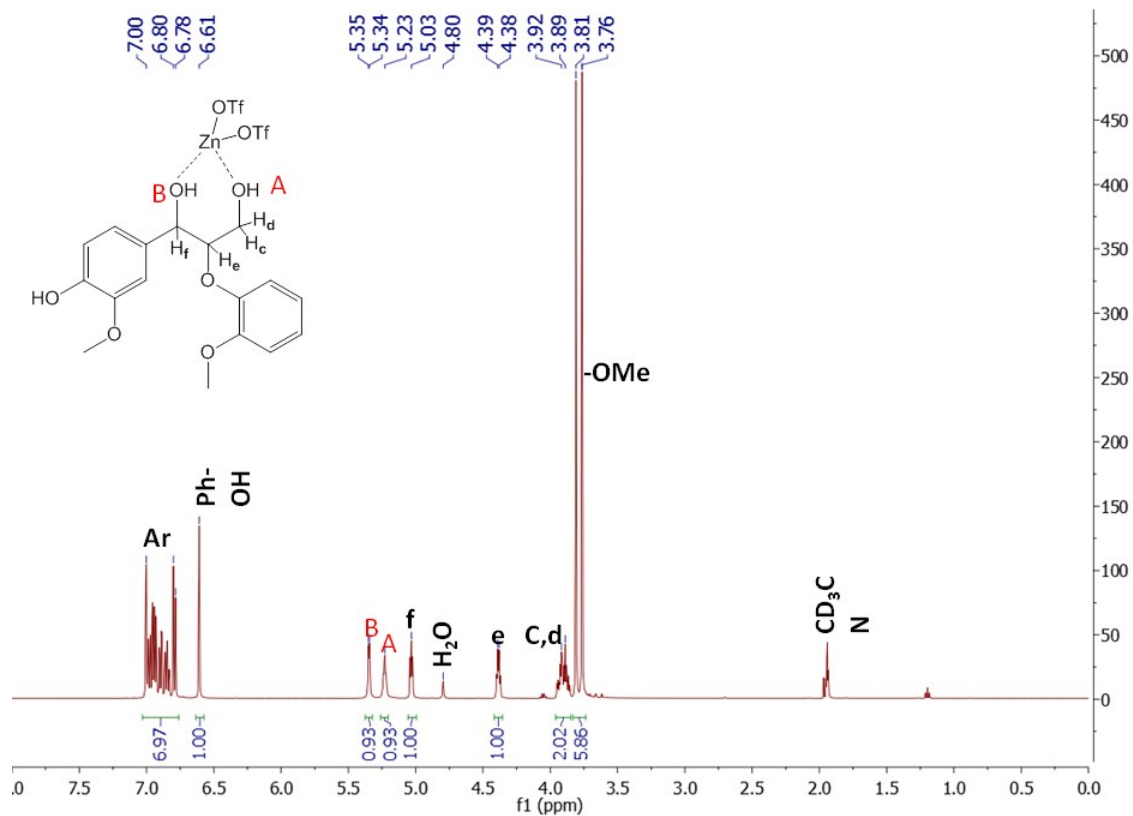


Figure S 19. ¹H NMR spectra of lignin model compound guaiacylglycerol- β -guaiacyl in CD₃CN, with 1 equivalent Zn(OTf)₂.

Table S1: Reaction of poplar biomass with Pd/C and Zn^{II} in ethanol solvent.

Entry	Catalyst	Co-catalyst	Molar Ratio Co-catalyst : Palladium	Yield (wt%)				Total Yield (wt%) ^a
				PG	PS	PG-OH	PS-OH	
1	Pd/C	Zn(OAc) ₂	2:1	16	28	8	-	44
2	Pd/C	-	-	10	17	17	18	53

Reaction conditions: milled poplar = 1.0 g, catalyst (5% Pd/C) = 0.01 g (10 wt%), co-catalyst varied according to listed molar ratio. T = 225 °C, 25 ml methanol, 500 psig H₂ and 12 h reaction time. ^a yields (%) are calculated from the theoretical lignin content in wood and the mass of the products quantified by GC-FID. Yields factor in the loss of two atoms of oxygen lost per each mole of products PG and PS produced, and one atom of oxygen lost per each mole of products PG-OH and PS-OH produced. Lignin content of poplar wood found to be 19% by DFRC (derivatization followed by reductive cleavage).

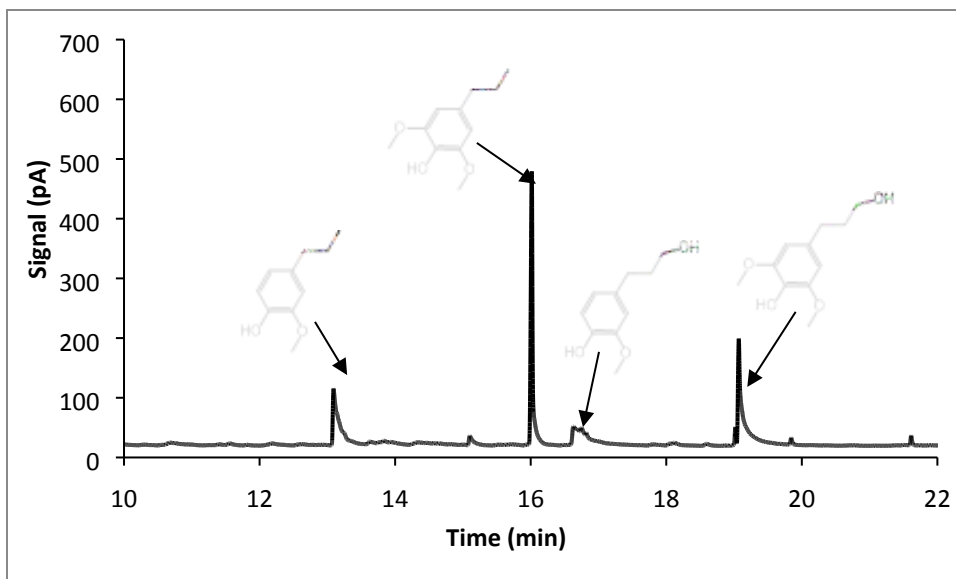


Figure S20. GC chromatogram of lignin catalysis products obtained from poplar wood using Pd/C catalyst in ethanol. Yields and reaction conditions reported in Table S1, entry 2.

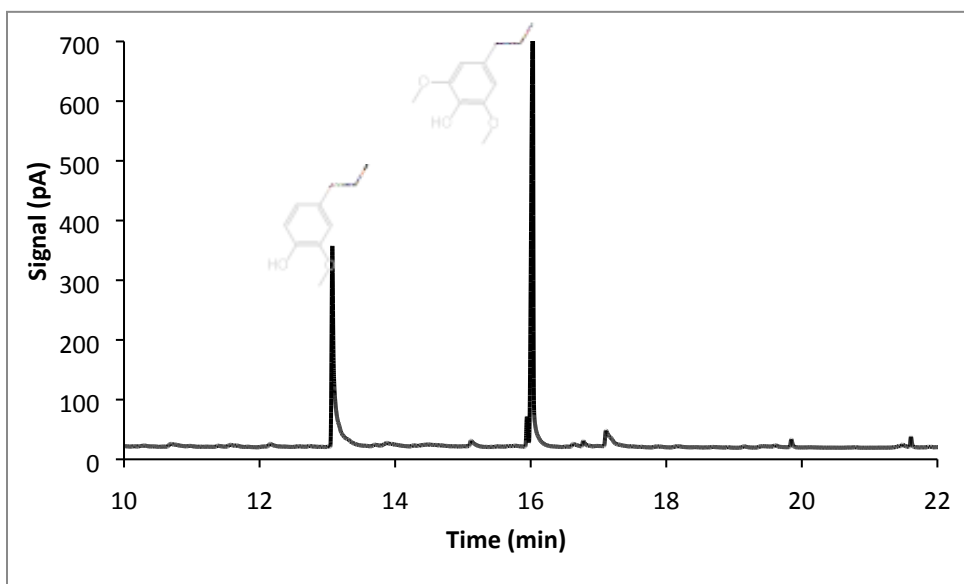


Figure S21. GC chromatogram of lignin catalysis products obtained from poplar wood using Zn/Pd/C catalyst in ethanol. Yields and reaction conditions reported in Table S1, entry 1.

Figure S22: Van't Hoff Plot for binding of OH-A of lignin model compound to Zn^{II}.

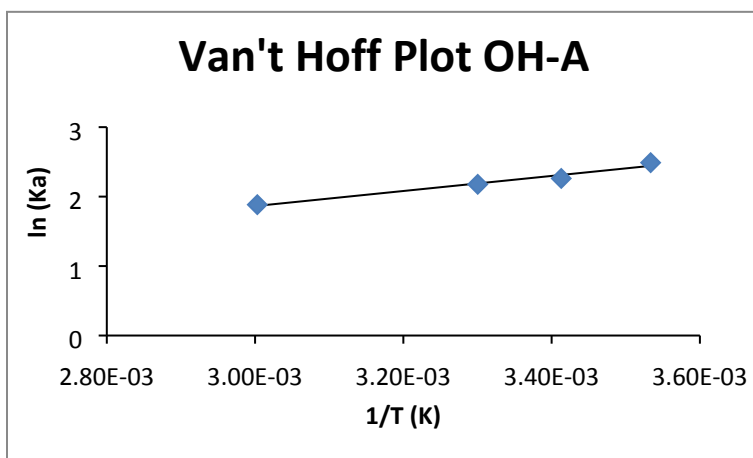
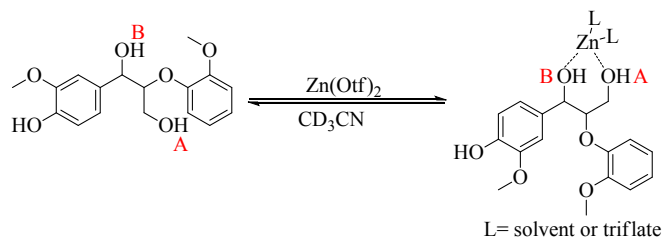


Figure S22: 0.0302 g (0.0944 mmol) lignin model compound 1 and 0.0171 g (0.0779 mmol) Zn(OTf)₂ dissolved in 0.75 mL CD₃CN. Solution was subjected to ¹HNMR and HMQC spectroscopy at temperatures of 10,20,30, and 60°C and the effect of temperature on the chemical shift of the hydroxyl proton OH-A was measured. Equation 1 ($\Delta\delta_L = \Delta\delta_{L_0} [Zn]/([Zn]+K_d)$) was used as described on page 4 of the main text to calculate K_a of OH(A). A Van't Hoff plot was generated by plotting ln(K_a) for the binding of OH(A) to Zn(OTf)₂ vs 1/T(K). From the slope of the Van't Hoff plot, $\Delta H = -9.07 \text{ kJ mol}^{-1}$ for the reversible binding of OH(A) to Zn^{II}. From the intercept of the Van't Hoff plot, $\Delta S = -11.6 \text{ J mol}^{-1} \text{ K}^{-1}$ for the reversible binding of OH(A) to Zn^{II}.

Figure S23: Van't Hoff Plot for binding of OH-B of lignin model compound to Zn^{II}.

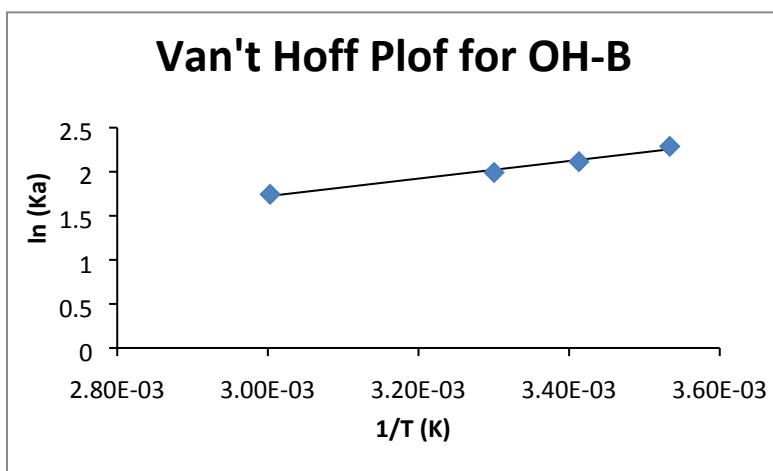
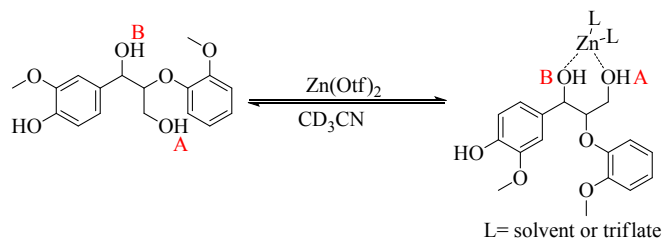


Figure S23: 0.0302 g (0.0944 mmol) lignin model compound 1 and 0.0171 g (0.0779 mmol) Zn(OTf)₂ dissolved in 0.75 mL CD₃CN. Solution was subjected to ¹HNMR and HMQC spectroscopy at temperatures of 10,20,30, and 60°C and the effect of temperature on the chemical shift of the hydroxyl proton OH-B was measured. Equation 1 ($\Delta\delta_L = \Delta\delta_{L_0} [Zn]/([Zn]+K_d)$) was used as described on page 4 of the main text to calculate K_a of OH(B). A Van't Hoff plot was generated by plotting ln(K_a) for the binding of OH(B) to Zn(OTf)₂ vs 1/T(K). From the slope of the Van't Hoff plot, $\Delta H = -8.3 \text{ KJmol}^{-1}$ for the reversible binding of OH(B) to Zn^{II}. From the intercept of the Van't Hoff plot, $\Delta S = -10.5 \text{ Jmol}^{-1}\text{K}^{-1}$ for the reversible binding of OH(B) to Zn^{II}.

Preparation of PG-diol (1-(4-hydroxy-3-methoxyphenyl)propane-1,3-diol)

1-(4-Benzyloxy-3-methoxyphenyl)propane-1,3-diol was synthesized according to literature procedures reported by Brandi et al, and characterized by ^1H NMR (Figure S 1).²⁵ The resulting tert-1-(4-Benzyloxy-3-methoxyphenyl)propane-1,3-diol was deprotected by stirring in a mixture of water and 1.0 M HCl (5:3 vol). Resulting crude product was purified on a short silica column (eluent: dichloromethane followed by methanol) to yield 1-(4-hydroxy-3-methoxyphenyl)propane-1,3-diol (45% yield). Characterization by ^1H and ^{13}C NMR (Figure S2, S3) was in agreement with previous reports.⁵³

Preparation of PS-OH (4-(3-hydroxypropyl)-2,6-dimethoxyphenol)

3,5-Dimethoxy-4-hydroxycinnamic acid, 2.490 g (11 mmol), was dissolved in 30 ml methanol and added to a stainless steel Parr vessel containing 0.2495 g of 5% Pd/C, pressurized with 500 psig H_2 , and heated to 200 °C for 12 hours. Reaction was cooled to ambient temperature, filtered, and reduced in vacuo to yield methyl 3-(4-hydroxy-3,5-dimethoxyphenyl)propanoate ^1H NMR (CDCl_3 , 500 MHz): δ 2.58 (2H, t, CH_2), δ 2.87 (2H, t, CH_2), δ 3.64 (3H, s, $-\text{OCH}_3$), δ 3.82 (6H, s, $-\text{OCH}_3$), δ 6.39 (2H, s, aromatic H). Methyl 3-(4-hydroxy-3,5-dimethoxyphenyl)propanoate, 0.4996 g (2.08 mmol), was dissolved in a 20 ml solution of 1:1 water and dioxane, to which 0.7873 g NaBH_4 (20.8 mmol) was added portionwise while stirring. Reaction was stirred under N_2 overnight, then quenched by dropwise addition of 15 ml HCl (1 M). Organic compounds were separated by addition of ethyl acetate, and washed with saturated NaBH_4 solution followed by brine. Organic compounds were then dried over Na_2SO_4 , filtered, and dried under vacuo to yield crude product. Crude product was purified on silica column (mobile phase 1:1 ethyl acetate and hexanes) to yield PS-OH (4-(3-hydroxypropyl)-2,6-dimethoxyphenol) (0.1611 g, 36% yield). ^1H NMR (CDCl_3 , 500 MHz): δ 1.84 (2H, m, CH_2), δ 1.94 (H, s, OH), δ 2.61 (2H, t, CH_2), δ 3.65 (2H, t, CH_2), δ 3.83 (6H, s, OCH_3), δ 5.58 (H, s, Ph-OH), δ 6.4 (2H, s, aromatic H).

HPLC/MS Analysis

Instrumentation. All analysis was performed using a Thermo Scientific linear quadrupole ion trap (LQIT) mass spectrometer coupled with a Surveyor Plus HPLC system consisting of a quaternary pump, autosampler, and photodiode array (PDA) detector. The mass spectrometer was equipped with an electrospray ionization (ESI) source. The eluent from the HPLC (flow rate 500 $\mu\text{L}/\text{min}$) was combined, via a T connector, with a 10 mg/mL sodium hydroxide in water solution (flow rate 0.2 $\mu\text{L}/\text{min}$) and then connected to the ion source. The sodium hydroxide solution allows for efficient negative ion generation by ESI.⁵¹ The LQIT was operated using the LTQ Tune interface and Xcalibur 2.0 software was used for HPLC/MS data analysis. A pressure of 0.80×10^{-5} , as read by an ion gauge, was maintained in the LQIT.

High-performance liquid chromatography/mass spectrometry. Samples were introduced into the HPLC/MS via an autosampler, utilizing a full loop (25 μ L) injection volume to ensure reproducibility. Water (A) and acetonitrile (B) were used as mobile phase solvents. The gradient used was as follows: initially 80% A and 20% B shifting to 50% A and 50% B at 20.0 minutes then shifting 20% A and 80% B at 55 minutes. The conditions used for ionization of the analytes and injection of the ions into the mass spectrometer were optimized using a stock solution of 2-methoxy-4-propylphenol in a 0.15 mg/mL NaOH 50:50 acetonitrile:water solution. All ion optics were optimized using the LTQ Tune automatic tuning feature. The following ESI conditions were used: sheath gas pressure 50 (arbitrary units), auxiliary gas pressure 30 (arbitrary units), sweep gas pressure 0 (arbitrary units) and spray voltage 3.50 kV. For the analysis of the observed products data-dependent scans were used. Data-dependent scanning allows the instrument to automatically select the most abundant ions present in order to analyze them further. These MS² experiments entail the isolation (using a mass/charge ration window of 2 Da) and fragmentation of the ions selected. The fragmentation was achieved by kinetically exciting the ions and allowing them to undergo collisions with helium for 30 ms at a q value of 0.25 and a normalized collision energy^{S2} of 40%. The most abundant product ions formed in the MS² experiments were then subjected to a further isolation and fragmentation (MS³).

References

- (S1) Hauptert, L. J.; Owen, B. C.; Marcum, C. L.; Jarrell, T. M.; Pulliam, C. J.; Amundson, L. M.; Narra, P.; Aqueel, M. S.; Parsell, T. H.; Abu-Omar, M. M.; Kenttämä, H. I. *Fuel* **2012**, *95*, 634–641.
- (S2) Lopez, L. L.; Tiller, P. R.; Senko, M. W.; Schwartz, J. C. *Rapid Commun. Mass Spectrom.* **1999**, *13*, 663–668.
- (S3) S. Ciofi-Baffoni, L. Banci, A. Brandi, *J. Chem. Soc., Perkin Trans. 1*, 1998, 3207-3218.